Regular Article

PHYSICAL CHEMISTRY RESEARCH
Published by the
Iranian Chemical Society
www.physchemres.org
info@physchemres.org

Phys. Chem. Res., Vol. 10, No. 2, 273-281, June 2022
DOI: 10.22036/pcr.2021.277674.1897

Interfacial Synthesis of Polyaniline-(Ag-Au) Alloy Nanocomposite

M.D. Bedre[a], V. Malashetty[b], R. Deshpande[c], S. Basavaraja[d], S. Ganiger[e] and A. Lagashetty[f,*]

[a]*Gurukul College of Science, Kalaburagi, 585102, Karnataka, India*
[b]*Department of Studies in Zoology, Vijayanagara Sri Krishnadevaraya University, Ballari, 583105, Karnataka, India*
[c]*H.K.E.S's College of Pharmacy, Kalaburagi, 585103, Karnataka, India*
[d]*Veeco-India Nanotechnology Laboratory, Jawaharlal Nehru Centre for Advanced Scientific Research, Bangalore, 5600016, Karnataka, India*
[e]*Department of Physics, Government Engineering College, Raichur, 584135, Karnataka, India*
[f]*Department of Studies in Chemistry, Vijayanagara Sri Krishnadevaraya University, Ballari, 583105, Karnataka, India*

(Received 14 March 2021, Accepted 5 November 2021)

(PANI)-(Ag-Au) alloy nanocomposites (ANC) were synthesized by an interfacial polymerization method using ammonium persulfate as oxidant at the water/chloroform interface. Ag^+ and Au^+ ions from the $AgNO_3$ and $HAuCl_4$ solutions were utilized in the formation of PANI-(Ag-Au) ANC. The structural variations of silver and gold incorporated PANI were confirmed by X-ray diffraction (XRD). Particle size and its distribution were determined from the transmission electron micrograph (TEM). The surface morphology and the bonding nature of the above-prepared sample were studied by scanning electron micrograph (SEM) and Fourier transform-infrared (FT-IR) respectively. The presence of Ag and Au metals in the sample was confirmed by EDX analysis. The thermal behavior of the alloy sample was studied by thermogravimetric analysis. The adsorption behavior of the sample for heavy metal ions, such as Pb^{2+} and Hg^{2+}, was determined by atomic absorption spectrometry (AAS). The results showed the considerable adsorption of heavy metal ions onto the ANC.

Keywords: Interfacial, Polyaniline, Nanocomposites, TEM, XRD, Thermogravimetric analysis

INTRODUCTION

Among conducting polymers, polyaniline (PANI) has become a particular focus of interest because of its environmental stability, controllable electrical conductivity [1], and interesting redox properties associated with the presence of nitrogen atoms. The electrical properties of the aniline polymers can be improved substantially by secondary doping [2]. PANI compounds can be designed to achieve the particular conductivity required for a given application. Incorporating nanosized metal particles into polymer matrices, such as polypyrrole (PPY) or PANI, is of current interest due to its promising applications [3-4]. On the one hand, the polymer can be used as a matrix to stabilize the growth of nanoparticles and prevent the agglomeration process. These stabilized nanoparticles are studied for their catalysis and optical, magnetic, mechanical, and electrical properties [5-6]. In addition, the nanoparticles can be incorporated into polymer matrices to enhance some of the polymer properties, such as conducting, structural, electronic, mechanical, and electrical properties [7-8]. Moreover, nanoparticles can serve as fillers to modify the polymer surface morphology or even print nanoelectronic circuits using some other templates or masks. Ag/Au

*Corresponding author. E-mail: arun.lagashetty@gmail.com

nanoparticles are known for their novel optical properties, surface-enhanced Raman scattering (SERS), and ability to attach biomolecules to be used as biosensors [9-11].

Recently, interfacial polymerization for the synthesis of PANI alloy nanocomposites has received attention from researchers due to its simplicity, eco-friendly nature, large-scale production ability, and potential to be used for the production of high-quality products with nanostructures [12-14]. Enhanced properties, such as electrical and electrochemical properties, have been observed in PANI composites compared to its plain PANI [15]. Dispersed metal/metal oxides in PANI are responsible for its conducting nature and act as pillars between the PANI chains. The electrochemical activity of PANI in its pure form is less due to the release of counter ions and its stability. A proper solution is to disperse metal/metal oxides in the PANI matrix [16].

Among various metal nanoparticles, Au-Ag bimetallic nanoparticles have several important applications in the field of biolabelling, sensors, antimicrobial agents [17-18], detection and destruction of cancer cells [19-20]. Several approaches have been proposed to embed the noble metal nanoparticles in various matrices, such as silica, alumina, borate glass, and MgO by sputtering, ion implantation, thermal vapor deposition, and a radio frequency magnetron co-sputtering method [21-22]. All these methods involve tedious procedures and adaptation. The aim of the present investigation was to report on the use of an interfacial polymerization method for the preparation of PANI-(Ag-Au) ANC by in situ chemical oxidation. The prepared alloy nanocomposite was characterized using various characterization techniques. The thermal and electrical properties of the ANC were studied in detail.

EXPERIMENTAL

Materials and Methods

Chemicals such as $AgNO_3$, $HAuCl_4$, ammonium persulphate (APS), HCl, and HNO_3 used in the present study were analytical grade reagents procured from Qualigens Chemicals Ltd. Double-distilled water and double-distilled aniline were also used in the experiment. The interfacial polymerization method was used for the preparation of PANI-(Ag-Au) ANC materials using chemical oxidation.

Synthesis of PANI-(Ag-Au) ANC

In a typical synthesis, 5 g of aniline is dissolved in 50 ml of chloroform ($CHCl_4$) in a separate beaker. 0.1 N $AgNO_3$ in 1 N HNO_3 and 0.1 N $HAuCl_4$ in 1 N HCl were prepared in two separate beakers. 0.1 N ammonium persulfate solution was prepared in distilled water in a separate beaker and used as an oxidizing agent in the polymerization reaction. These three mixtures were slowly added to the organic phase, containing aniline and chloroform, by maintaining the temperature between 0-5 °C. After 5 min, a blackish green-colored material was formed slowly at the interface (Fig. 1). Then, the reaction content was kept for 24 h. After complete oxidation of PANI with Ag-Au sample, the entire aqueous phase was filled homogeneously with blackish green PANI-(Ag-Au) ANC. The aqueous phase was then collected and washed with ethanol, followed by water, to remove the unreacted aniline. The residue obtained PANI-(Ag-Au) ANC was purified and was dried in a vacuum oven at 40 °C for 36 h [23-24]. The powder form of the sample is shown in Fig. 2a.

Preparation of Pellets

The powder of PANI-(Ag-Au) ANC obtained using the interfacial synthesis method was crushed and ground finely in the presence of acetone medium in an agate mortar. The powder was pressed to form pellets of 10 mm diameter and

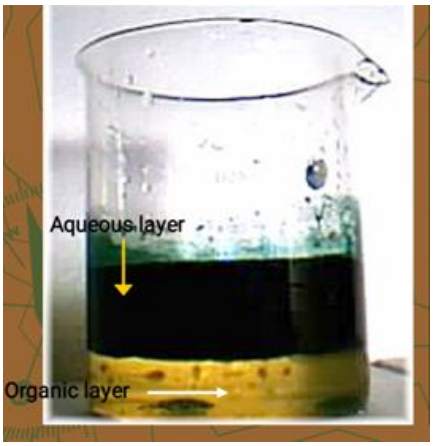

Fig. 1. The interface formation of PANI-(Ag-Au) ANC.

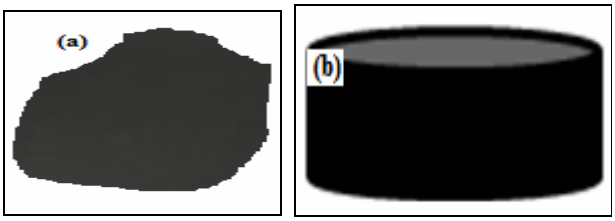

Fig. 2. (a) Prepared PANI-(Ag-Au) ANC, (b) Magnified PANI-(Ag-Au) ANC pallet.

its thickness varied from 1 to 2 mm under an applied pressure of 90 MPa in a hydraulic press [25]. The optical image of the magnified PANI-(Ag-Au) ANC pallet is shown in Fig. 2b.

Adsorption Study

First, 200 ppm of lead acetate solution was prepared in double-distilled water, and 20 ml of the solution was taken in a conical flask containing 1 g of the prepared PANI-(Ag-Au) ANC sample. The solution was well shaken on a mechanical shaker of 300 rpm for about 5 h for the adsorption process. Then, the solution was kept constant for one h for complete adsorption. The eluent solution was taken out and subjected to atomic absorption spectroscopy (AAS). The adsorbed powder ANC sample was dried at room temperature and subjected to various characterizations to study the adsorption of lead ions on the adsorbent sample. A similar procedure was carried out for mercury metal ions on the PANI-(Ag-Au) ANC sample

Characterization Techniques

The crystallinity of conducting polymers is a matter of interest due to their highly ordered systems exhibiting high conductivity. Thus, to examine the crystallinity of the sample, the ANC was exposed to X-ray diffraction (XRD) analysis. The powder XRD patterns of the sample were recorded on a JEOL JDX-8P diffractometer using CuK_{α} radiation (1.5406 Å) at 30 kV.

The chemical bonding state of the ANC was systematically investigated using Fourier transform-infrared (FT-IR) spectra. The surface functional groups were verified, and the structural information on all nanocomposite materials as well as the transmittance of polyaniline in the ANC were identified by FT-IR spectral analysis. FT-IR spectra of the prepared ANC samples were recorded on a Perkin-Elmer FT-IR spectrometer (Model No. 1000) in the range of 4000-400 cm^{-1} at a resolution of 4 cm^{-1}. The IR spectra of the samples were recorded at room temperature in the mid-IR region of 4000-400 cm^{-1}.

Thermogravimetric analysis (TGA) of the sample was performed using a NETZSCH STA 409 PC instrument. TGA data were obtained at a heating rate of 10 °C min^{-1} under argon atmosphere.

Transmission electron microscopy image was obtained using a JEOL 100CX operated at 190 KeV. The sample was drop-coated on carbon-coated copper grids, which had been placed on blotting paper, and then allowed to dry in air for 5 min.

The performance of ANC in aqueous medium was assessed based on the collection of several PANI chains and an electronic combination of pi-system. The transition of charge transporters was examined by UV-Vis spectrum. The absorption behavior of the sample was examined by UV-Vis spectrophotometric measurements using the Elico spectrophotometer. The required amount of diluted supernatant sample was placed in a quartz cuvette with a 1 nm path length and inserted in a UV-Vis spectrophotometer in the short wavelength range of 300-700 nm to obtain the UV-Vis spectra of the prepared sample. The sample was ultrasonicated just before the UV-Vis studies were performed to confirm uniform distribution.

To study the particle morphology, the metal sample was analyzed using a JEOL JSM-6380 LA Scanning electron microscope with energy dispersive analysis of X-Ray (EDAX).

The concentrations of lead and mercury solution before and after the adsorption of the ANC were determined by atomic absorption spectrometry. This analysis was recorded on a Smith-Hieftje 1000 automated AA/AE spectrometer.

RESULTS AND DISCUSSION

X-ray Diffraction (XRD)

Figure 3 shows the XRD pattern of PANI-(Ag-Au) ANC synthesized by interfacial polymerization. The pattern shows the presence of Bragg reflections due to the crystalline nature of the sample. Most of the peaks observed and indexed in the pattern are related to Ag-Au

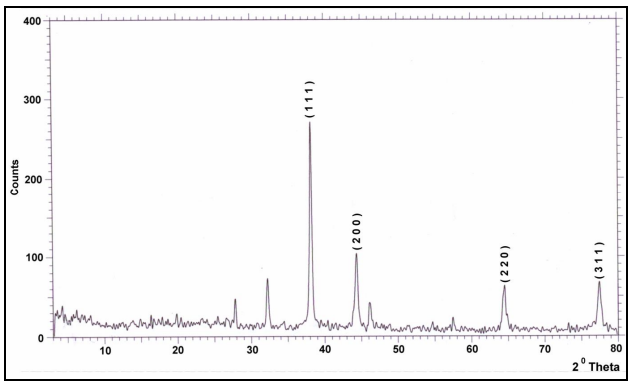

Fig. 3. The obtained XRD pattern for PANI-(Ag-Au) ANC.

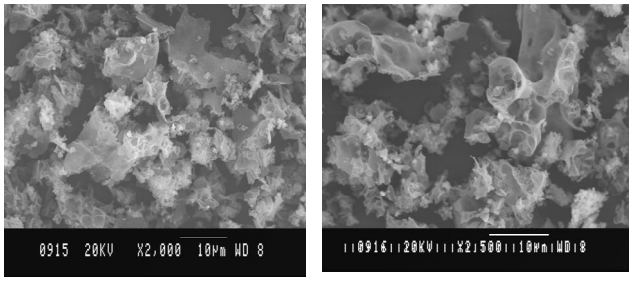

Figs. 4a-b. The SEM image of PANI-(Ag-Au) ANC at low and high magnifications.

nanoparticles. The obtained d-spacing values of the sample matched well with the JCPDS file of Ag and Au (04-0783 and 01-1174), respectively. The peaks obtained for alloy nanoparticles were also observed at the same 2θ values in the Ag and Au patterns [26-28]. The mean particle diameter was calculated from the XRD pattern based on the high-intensity diffraction peaks and using the Debye-Scherrer equation:

$$D = \frac{K\lambda}{\beta_{1/2}\cos\theta}$$

where lambda is the X-ray wavelength (1.5418), $\beta_{1/2}$ is the width of the XRD peak at half height, and K is the shape factor. In addition, this equation uses the reference peak width at an angle θ. The mean particle diameter of PANI-(Ag-Au) ANC was calculated using the Debye-Scherrer equation, and it was found to be 80 nm, which is in partial agreement with the TEM results.

Scanning Electron Microscopy (SEM)

In our earlier work, we presented the morphology of plain PANI by SEM image. In the present study, that image was considered as the control image of PANI-(Ag-Au) ANC. The SEM image revealed the semi-crystalline nature of the sample with heterogeneity [29]. Figures 4a and 4b show the typical SEM image of the as-synthesized PANI-(Ag-Au) ANC at low and high magnifications, respectively. It can be observed from the SEM images that the distribution of metal particles is agglomerated due to the formation of matrix mixing or close complexation. The more aggregation of the particles in the image can be attributed to the metal matrix in PANI. The varied particles with irregular shapes observed in the image can be due to the complexed metals matrix mixing and the enhanced crystallinity of the PANI. In short, the image illustrates the difference between the morphology of PANI-(Ag-Au) ANC and that of plain PANI. This change in morphology can be attributed to the interaction between PANI and metal alloy nanoparticles.

Transmission Electron Microscopy (TEM)

Figure 5 shows the typical bright-field TEM image of the as-synthesized PANI-(Ag-Au) ANC. It can be seen from the image that the distribution of alloy nanoparticles is polydispersed in the polymer matrix and that the particles are of different sizes. The image reflects spherical structures, and the spherical aggregates composed of dark spots symbolize the metal nanoparticles encapsulated with the PANI matrix. In addition, most of the particles were found to be spherical and hexagonal in shape, which is in agreement with the result obtained from the Scherrer equation of XRD. Furthermore, the TEM image of the PANI-(Ag-Au) ANC sample shows that the Ag-Au nanoparticles were finely dispersed into the polymer matrix. This can be attributed to the intense turbulence and micro-mixing caused by polymerization. Also, the size of particles suggests that the composites obtained were nanostructured. The metal nanoparticles seemed to be embedded in the PANI matrix and started to coalesce and form agglomerates due to the absorption property of PANI. The change in morphology can be explained by the absorption and intercalation of PANI on metal alloys.

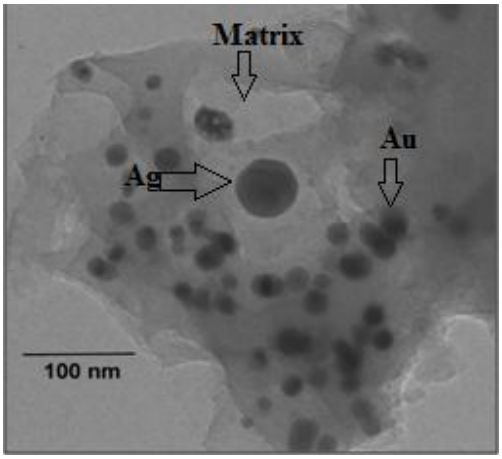

Fig. 5. The TEM image of the as-synthesized PANI-(Ag-Au) ANC.

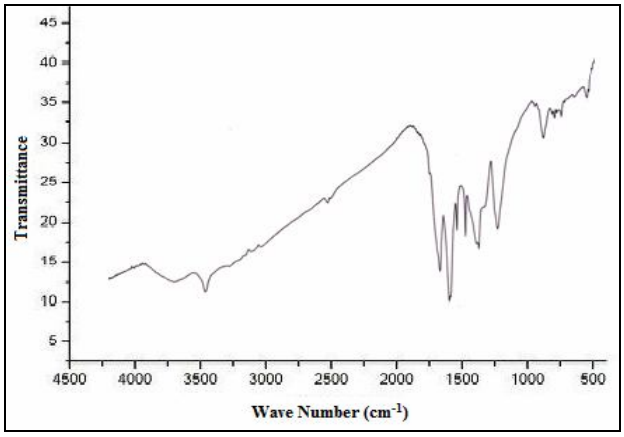

Fig. 6. The FT-IR spectra of the PANI-(Ag-Au) ANC sample.

Fourier Transform-Infrared (FT-IR) Spectroscopy

Figure 6 shows the FT-IR spectra of plain PANI and PANI-(Ag-Au) ANC polymer nanocomposite samples, respectively. The bands at 1563 and 1481 cm^{-1} are attributed to the C=N and C=C stretching mode of vibration for the quinonoid and benzenoid units of PANI. The peaks at 1300 and 1236 cm^{-1} are assigned to the C–N stretching mode of the benzenoid ring. The peak at 1239 cm^{-1} is the characteristic of the conducting protonated form of PANI. The bands in the region of 1000-1110 cm^{-1} are assigned to in-plane bending vibration of C–H mode. The band at 820 cm^{-1} originates out-of-plane C–H bending vibration.

Moreover, Fig. 6 shows two additional peaks at 665 and 703 cm^{-1}, which are due to the presence of metal complexation in PANI. On both spectra, some bands shifted slightly compared with the reported PANI, indicating that some interactions such as weak Vander Waals forces of attraction may have existed between PANI and the metals [30].

Thermal Study

Figure 7 shows the TGA curve of as prepared PANI-(Ag-Au) ANC. The curve shows that multistep continuous weight loss occurred from room temperature to 450 °C. These weight losses appeared as exothermic peaks at 75, 300, and 450 °C, respectively. The exothermic peak at 75 °C is attributed to the loss of adsorbed water molecules,

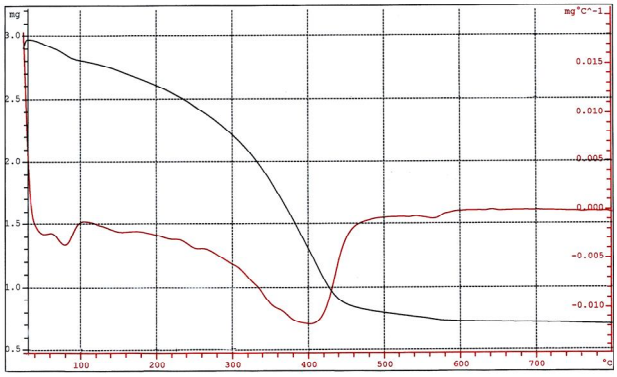

Fig. 7. The TGA trace of the PANI-(Ag-Au) ANC sample.

and other exothermic peaks correspond to the decomposition of the sample. The endothermic process happened at nearly 450 °C, which corresponds to the formation and transition of the crystalline phases. The thermal decomposition of the sample had more stability compared to plain PANI; this may be due to the loss of Ag-Au nanoparticles from the PANI matrix. It may be concluded that the incorporation of Ag-Au nanoparticles into PANI enhanced the thermal stability of the polymer, indicating an interaction between Ag-Au nanoparticles and the PANI matrix. This is in line with a broad peak observed in the DTA trace at around 410 °C. The exothermic and endothermic regions in the DTA pattern are consistent with the change regions in the TG pattern. The TG curve shows

no further weight loss above 500 °C, confirming the formation of a stable alloy composite material.

Energy-Dispersive X-ray (EDX) Microanalysis

The results of EDX show the elements present in the ANC sample. The EDX analysis of the PANI-(Ag-Au) ANC was performed to confirm the incorporation of the Ag and Au nanoparticles into the PANI matrix. Figure 8 shows the EDX pattern of as-synthesized PANI-(Ag-Au) ANC nanocomposite sample. A profile of the dispersed metal showed a strong atomic signal, indicating the crystalline nature of the sample. The optical absorption peak occurred at 2 keV while the typical absorption of Au and Ag nanoparticles was observed at 3 keV in the pattern. The presence of a strong signal of Au and Ag atoms in the PANI matrix confirmed the formation of PANI-(Ag-Au) ANC. No other signals except that of Ag and Au in the pattern indicated the purity of the sample.

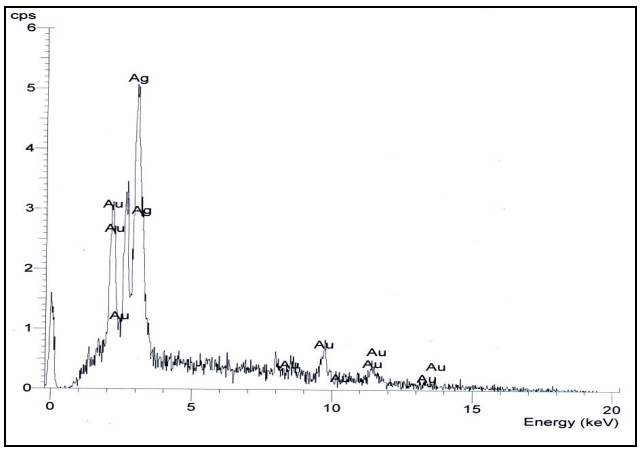

Fig. 8. The EDX pattern of PANI-(Ag-Au) ANC.

Electrical Conductivity Study

Figure 9 shows the electrical conductivity graph of the interfacial polymerized PANI-(Ag-Au) ANC sample. It is clear from the figure that the increase in conductivity led to an increase in temperature. More specifically, the conductivity increased slightly in the sample when the temperature increased up to 180 °C; however, a sudden increase was observed in conductivity when the temperature exceeded 180 °C. This kind of increase in conductivity in the order of 10^{-2} s cm^{-1} can be due to the doped Ag and Au in the PANI matrix.

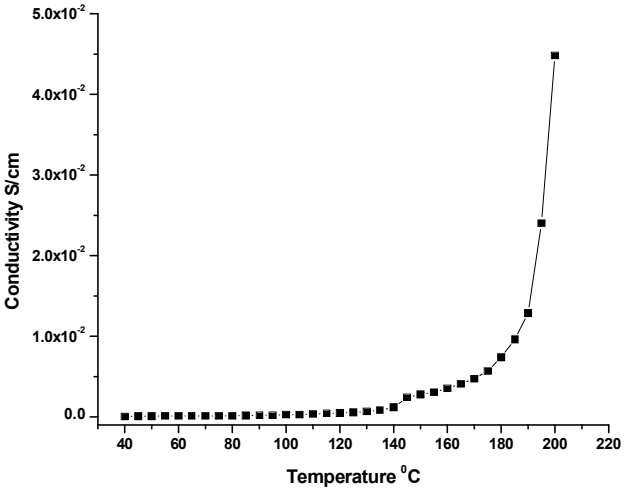

Fig. 9. The Electrical conductivity of PANI-(Ag-Au) ANC.

UV-Vis Study

Figure 10 shows the UV-Vis spectrum of PANI-(Ag-Au) ANC formed in the aqueous phase. The absorption band at 430 nm is attributed to the excitation from the highest occupied molecular orbital of the benzenoid π-π interactions to the lowest unoccupied molecular orbital of the localized quinoid ring and the two surrounding imine nitrogens in the PANI. Furthermore, Ag-Au nanoparticles were dispersed in the PANI matrix, leading to a significant change in the absorption spectrum. The formation of an absorption band at 430 nm for the PANI-(Ag-Au) ANC sample continued to extend to the near-IR region, indicating the formation of oligomers in the doped state [31-32].

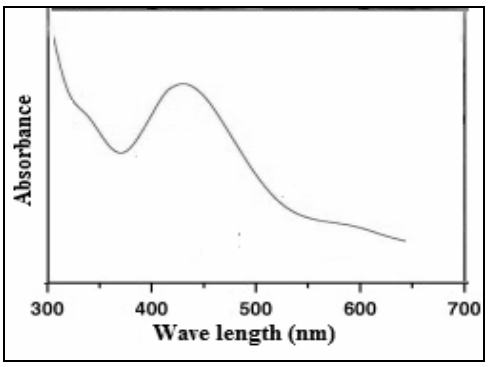

Fig. 10. The UV-Vis spectra of the PANI-(Ag-Au) ANC sample.

Table 1. The AAS Results of Lead and Mercury Adsorption on PANI-(Ag-Au) ANC Sample

Sl. No	Concentration	Concentration of Pb^{2+} solution	Concentration of Hg^{2+} solution
1	Initial concentration	300	300
2	Concentration after passing through the PANI-(Ag-Au) ANC sample	140	130

Adsorption Study

Table 1 shows the AAS results of pure lead and mercury solutions with eluent lead and mercury solutions after adsorption. The reduction in the concentration of eluent lead and mercury solutions compared with that of plane lead and mercury solutions, as clearly shown in Table 1, reflects the loss of lead and mercury ions by adsorption on the PANI-(Ag-Au) ANC sample [33]. The PANI-(Ag-Au) ANC sample showed considerable adsorption due to the remarkable adsorption active sites present on the sample. The adsorption study revealed that the prepared composite sample could act as a good adsorbent for heavy metal ions.

CONCLUSIONS

The preparation of PANI-(Ag-Au) ANC was achieved by interfacial polymerization of aniline. SEM showed the formation of clusters, and TEM showed the incorporation of spherical-shaped Ag-Au particles into the PANI. The evidence from the EDX and XRD indicated that there was an interaction between the PANI and alloy (weak Vander Waals forces of attraction). The results also showed a reduction in Ag and Au during polymerization. The TG analysis revealed that the thermal stability of PANI-(Ag-Au) ANC composites was higher than that of pure PANI. This can be attributed to the interaction between PANI and Ag-Au alloy. These findings have several important applications in the field of biolabelling, sensors, antimicrobial agents, and the detection and destruction of cancer cells.

ACKNOWLEDGMENTS

The authors would like to express their gratitude for the DST-FIST (SR/FST/CSI-003/2016) grant, which provided Vijayanagara Sri Krishnadevaraya University, Ballari, with the necessary instruments and infrastructure facilities. We also would like to thank Professor A. Venkataraman, Department of Chemistry, Gulbarga University, Kalaburagi, Karnataka, India, for his useful comments on spectral analysis.

REFERENCES

[1] Prasanna, B. P.; Avadhani, D. N.; Muralidhara, H. B.; Chaitra, K.; Vinny R. T.; Revanasiddappa, M.; Kathyayini, N.; Synthesis of polyaniline/ZrO_2 nanocomposites and their performance in AC conductivity and electrochemical sup.; Omnia, er capacitance, Bull. Mater. Sci., **2016**, *39*, 667-675, DOI: 10.1007/s12034-016-1196-9.

[2] Abdel, F. D.; Ahmed, G.; Mohamed, Y. H. E. S.; Shehata, Gamal, T.; Synthesis and characterization of polyaniline/Mn_3O_4/reduced graphene oxide nanocomposite, *Egy. J. Chem.* **2019**, *62*, 251-265, DOI: 10.21608/ejchem.2019.13194.1821.

[3] Saira, I.; Mahmoud, M.; Farah, K.; Muhammad, E.; Muhammad, S.; Truc, N. V.; Dusan, L.; Facile synthesis of ternary graphene nanocomposite with doped metal oxide and conductive polymers as electrode materials for high performance supercapacitors, Sci. Rep., 2019, 9, 5974. DOI: 10.1038/s41598-019-41939-y.

[4] Sampreeth, T.; Al-Maghrabi, M. A.; Bahuleyan, B. K.; Ramesan, M. T.; Synthesis, characterization, thermal properties, conductivity and sensor application study of polyaniline/cerium-doped titanium dioxide nanocomposites, *J. Mater. Sci.* **2018**, *53*, 1-26, DOI: 10.1007/s10853-017-1505-8.

[5] Fan, Z.; Huaqiang, C.; Dongmei Y.; Jingxian, Z.; Meizhen, Q., Enhanced anode performances of

polyaniline-TiO_2-reduced graphene oxide nanocomposites for lithium ion batteries, *Inorg. Chem.* **2012**, *51*, 9544-9551, DOI: 10.1021/ic301378j.

[6] Shun-J, L.; Hong-Juan, S.; Tong-J, P.; Linn-H, J.; Synthesis of high-performance Polyaniline/graphene oxide nanocomposites, *High Perform. Polym.* **2014**, *26*, 790-797, DOI: 10.1177/ 0954008314529982.

[7] Harish, K.; Anurag, B.; Ankita, Y.; Rajni, R.; Polyaniline-metal oxide-nano-composite as a nano-electronics, opto-electronics, heat resistance and anticorrosive material, *Res. in Chem.* **2020**, *2*, 100046, DOI: 10.1016/j.rechem.2020.100046.

[8] Manjunatha, B.; Arjun, N.; Shetty, Kaveri, S.; Sundar, S.; Mety, K. C.; Anjaneya, Ramakrishna, R., Sangshetty, K.; Chemical mediated synthesis of polyaniline/tungsten oxide (PANI/WO_3) nanocomposites and their antibacterial activity against clinical pathogenic bacteria, *Bio. Nano Sci.* **2020**, *10*, 73-80, DOI: 10.1007/s12668-019-00679-z.

[9] Tanushree, S.; Satyendra, M.; Navinchandra, G.; Shimpi, Synthesis and sensing applications of polyaniline nanocomposites: a review, *RSC Adv.,* **2016**, *48*, 42196-42222, DOI: 10.1039/c6ra03049a.

[10] Lida, A.; Ebrahim, M.; Samaneh, G.; Roghayeh, B.; Hamidreza Pazoki-Toroudi,; Soodabeh Davaran,; Development and characterization of a novel conductive polyaniline-g-polystyrene/Fe_3O_4 nanocomposite for the treatment of cancer, artificial cells, nanomedicine, and biotechnology, *An Intenl. J.,* **2019**, *47*, 873-881, DOI: 10.1080/ 21691401.2019.1575839.

[11] Ameena, P.; Raghunandan, D.; Shakeel, A.; Aashis, R., Synthesis, characterization, and DC conductivity of polyaniline-lead oxide composites, *Chem. Papers*, **2013**, *67*, 350-356, DOI: 10.2478/s11696-012-0270-z.

[12] Patil, R.; Roy, A. S.; Anilkumar, K. R.; Ambika, Prasad, M. V. N.; Ekhelikar, S., Electrical Conductivity of polyaniline/$NiZnO_3$ composites, A solid state electrolyte. *Ferroelectric*, **2011**, *423*, 77-85, DOI: 10.1080/00150193.2011.620836.

[13] Lagashetty, A.; Sangappa, K.; Ganiger,; Synthesis, characterization and antibacterial study of Ag-Au bi-metallic nanocomposite by bio reduction using piper betal leaf extract, *Heliyon*, **2019**, *5*, e02794. DOI: 10.1016/j.heliyon.2019.e02794.

[14] Genilson, R. D. S.; Vicente, L. K.; Murilo, P. M.; Magno, A.; Gonçalves, T.; Nelson, L.; de Campos Domingues,; Andrelson Wellington Rinaldi,; One-step electrochemical synthesis of polyaniline/metallic oxide nanoparticle (γ-Fe_2O_3) thin film. *Int. J. Electrochem. Sci.,* **2016**, *11*, 5380-5394. DOI: 10.20964/2016.07.39.

[15] Zha, D.; Xiong, P.; Wang, X., Strongly coupled manganese ferrite/carbon black/polyaniline hybrid for low-cost super capacitors with high rate capability. *Electrochem. Acta*, **2015**, *185*, 218-228, DOI: 10.1016/j.electacta.2015.10.139.

[16] Moyseowicz, A.; Śliwak, A.; Miniach, E.; Gryglewicz, G., Polypyrrole/iron oxide/reduced graphene oxide ternary composite as a binderless electrode material with high cyclic stability for supercapacitors. *Compos. B. Eng,*, **2017**, *109*, 23-29. DOI: 10.1016/j.compositesb.2016.10.036.

[17] Wang, W.; Hao, Q.; Lei, W.; Xia, X.; Wang, X., Ternary nitrogen-doped graphene/nickel Ferrite/ polyaniline nanocomposites for high-performance super capacitors. *J. Power Sources*, **2014**, *269*, 250-259, DOI: 10.1016/j.jpowsour.2014.07.010.

[18] Lagashetty, A.; Manjunath, K. Patil,; Sangappa K. Ganiger,; Green synthesis, characterization, and thermal study of silver nanoparticles by achras sapota, psidium guajava, and azadirachtaindica plant extracts, *Plasmonics*, **2019**, *14*, 1219-1226, DOI: 10.1007/ s11468-019-00910-3.

[19] Bashir, T.; Shakoora, E.; Ahmeda, N.; Niaza, A.; Muhammad, S. A.; Muhammad, R. R.; Mohammad, A. M.; Peter, J.; Foot, S., Polypyrrole-Fe_2O_3 nanocomposites with high dielectric constant: *In situ* chemical polymerization, *Polym. Polym. Compos*., **2018**, *26*, 233-241. DOI: 10.1177/ 096739111802600303.

[20] Shumaila, D.; Zulfequar, M.; Husain, M., Synthesis, characterization and properties of MgB_2 doped polyaniline, *J. Mod. Mater*, **2017**, *4*, 1-9, DOI: 10.21467/jmm.4.1.1-9.

[21] Mahesh, D. B.; Basavaraj, S.; Balaji, S. D.; Shivakumar, V.; Lagashetty, A.; Venkataraman, A., Preparation and characterization of polyaniline and

polyaniline-silver nanocomposites *via* interfacial polymerization. *Polym. Compos*., **2009**, *30*, 1668-1677, DOI: 10.1002/pc.20740.

[22] Basavaraj, S.; Balaji, S. D.; Mahesh, D. B.; Lagashetty, A.; Vijayanand Havanoor,; Venkataraman, A., Use of liquid-liquid interfacial for synthesis of amorphous maghemite nanoneedles. *Surf. Rev. Lett*., **2012**, *19*, 50019, DOI: 10.1142/S0218625X12500199.

[23] Manawwer, A.; Naser, M.; Alandis,; Anees, Ansari, A.; Mohammed, R. S., Optical and electrical studies of polyaniline/ZnO nanocomposite, *J. Nanomater*., Article ID 157810, **2013**, 1-5, DOI: 10.1155/2013/157810.

[24] Mallikarjuna, N.; Nadagouda,; Rajender S.; Varma,; Green synthesis of silver and palladium Nanoparticles at room temperature, using coffee and tea extract, *Green Chem.,* **2008**, *10*, 859- 868. DOI: 10.1039/B804703K.

[25] Ramakritinan, C. M.; Kaarunya, E.; Sugandha, S.; Kumaraguru, A. K., Antibacterial effects of Ag, Au and bimetallic (Ag-Au) nanoparticles synthesized from red algae, *Solid State Phenom.,* **2013**, *201*, 211-230, DOI: 10.4028/ www.scientific.net/SSP.201.211.

[26] Ravikiran, Y. T.; Lagare, M. T.; Sairam, M.; Mallikarjuna, N. N.; Sreedhar, B.; Manohar, S.; MacDiarmid, A. G.; Aminabhavi, T. M., Synthesis, characterization, low frequency AC conduction of polyaniline/niobium pentoxide composites, *Synth. Met.*, **2006**, *156*. 1139-1147, DOI: 10.1016/j.synthmet.2006.08.005.

[27] Lagashetty, A.; Amruta, P.; Sangappa, K. G., Synthesis, characterization and antibacterial study of Ag doped magnesium ferrite nanocomposite, *Heliyon*, **2019**, *5*, e01760, DOI: 10.1016/ j.heliyon.2019.e01760.

[28] Nurul, H. I. H.; Mohd Kamarul, Z. M.; Saliza, A., Synthesis of PANI/iron(II,III) oxide hybrid nanocomposites using sol gel method, *J. Sci. Tech*., **2018**, *10*, 1-4. DOI: 10.30880/jst.2018.10.01.001.

[29] Mahesh, D.; Bedre, Basavaraj, S.; Balaji, S. D.; Shivakumar, V.; Arunkumar Lagashetty; Venkataraman, A., Preparation and characterization of polyaniline and polyaniline-silver nanocomposites *via* interfacial polymerization, *Polym. Compos.,* **2009**, *30*, 1668-1677.

[30] Lagashetty, A.; Sangappa, K. G.; Preeti, R. K.; Shashidhar, R., Green synthesis, characterization and antibacterial study of Ag-Au bimetallic nanocomposite using tea powder extract, *Biointerface Res. Appl. Chem*., **2021**, *11*, 8087-8095. DOI: 10.33263/BRIAC111.80878095.

[31] Bharati, N.; Subhash, K.; Mahesh, S., Nanostructure cobalt oxide reinforced conductive and magnetic polyaniline nanocomposites, *J. Compos. Mater.***, 2013**, *47*, 559-567. DOI: 10.1177/0021998312442559.

[32] Sangappa, K. G.; Murugendrappa, M. V., Lab scale study on humidity sensing and D.C. conductivity of polypyrrole/strontium arsenate ($Sr_3(AsO_4)_2$) ceramic composites, *Polym. Sci. Ser. B*, **2018**, *60*, 395-404, DOI: 10.1134/S1560090418030119.

[33] Natraj, H.; Rangappa, D.; Lagashetty, A., Synthesis and characterization of $LiMnPO_4$/carbon nanocomposite material as cathode materia, *Phys. Chem. Res.,* **2016**, *4*, 285-289, DOI: 10.22036/pcr.2016.14079.